

Supporting Information for

Interfacial Insights for Divergent Dendrite  
Formation Mechanisms in Lithium and Magnesium  
Anodes

*Hong-Kai Chen,<sup>a</sup> Hong-Kang Tian<sup>a,b,c,\*</sup>*

<sup>a</sup> Department of Chemical Engineering, National Cheng Kung University, No. 1 University Road,  
Tainan City 70101, Taiwan

<sup>b</sup> Program on Smart and Sustainable Manufacturing, Academy of Innovative Semiconductor and  
Sustainable Manufacturing, National Cheng Kung University, Tainan 70101, Taiwan

<sup>c</sup> Hierarchical Green-Energy Materials (Hi-GEM) Research Center, National Cheng Kung  
University, Tainan 70101, Taiwan

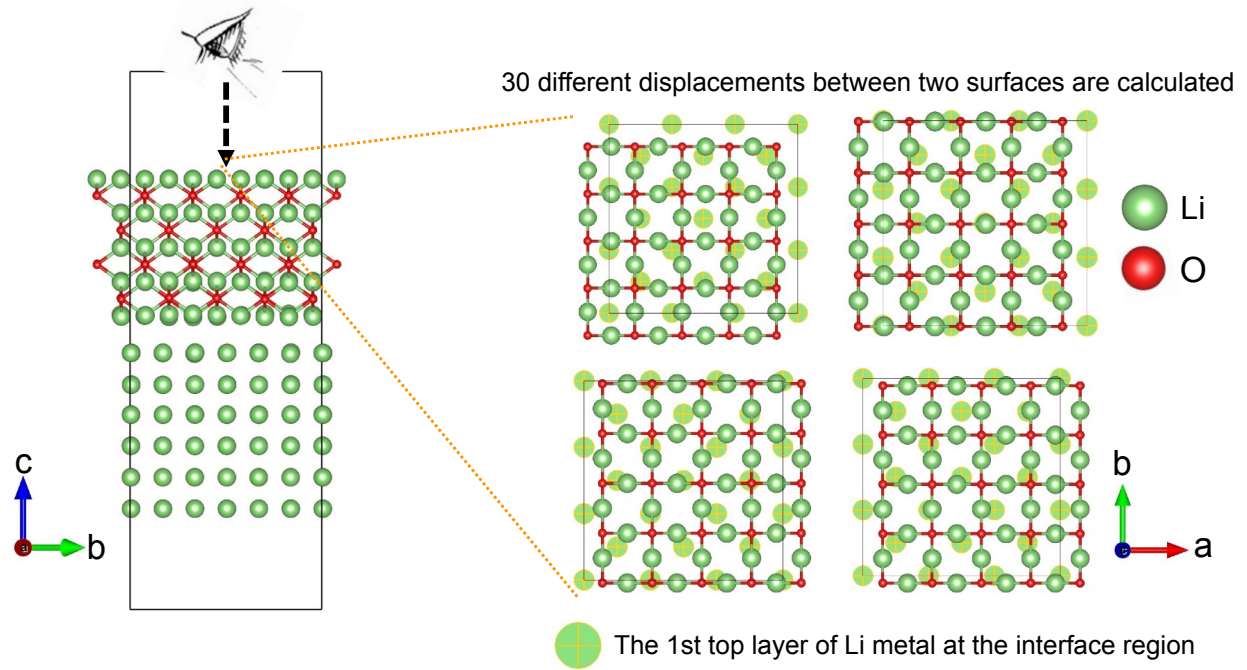


**Figure S1.** The schematic of the displacement between two surfaces in a heterogeneous interface model.

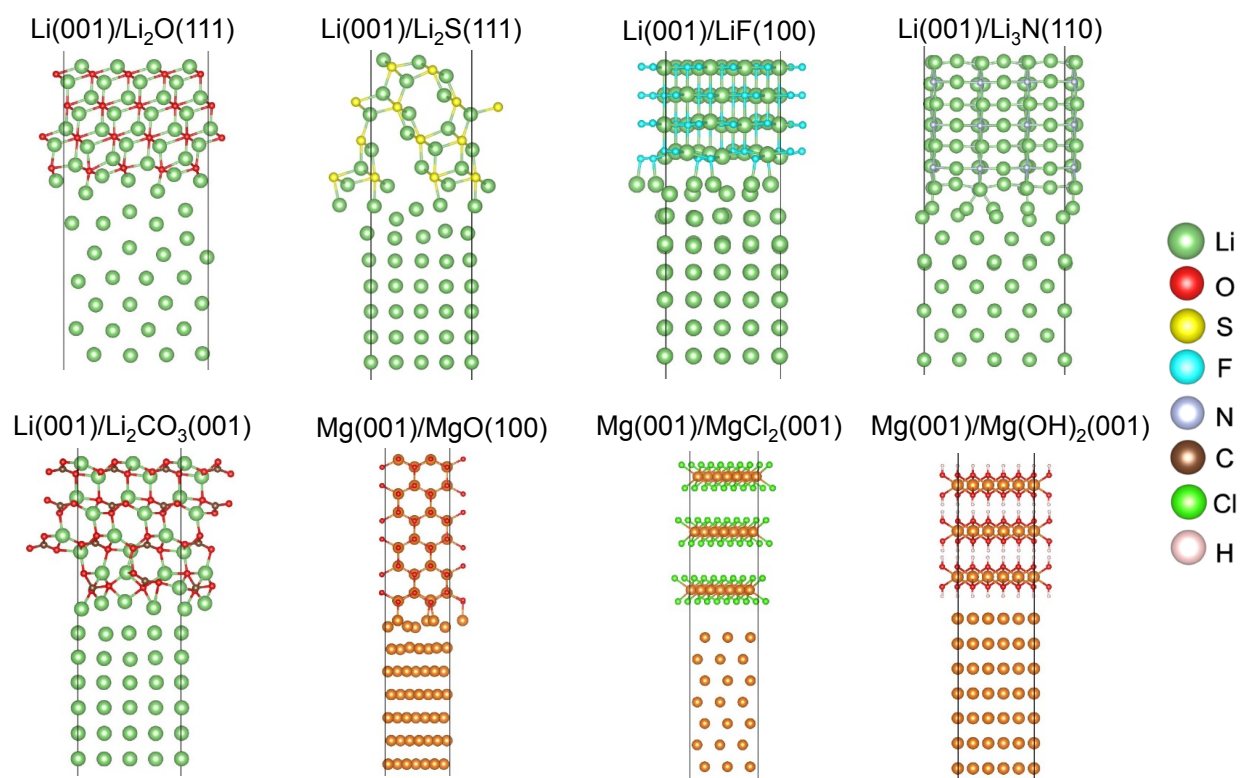


**Figure S2.** Density Functional Theory (DFT)-optimized interface structures, which are constructed using surfaces with the lowest surface energy.

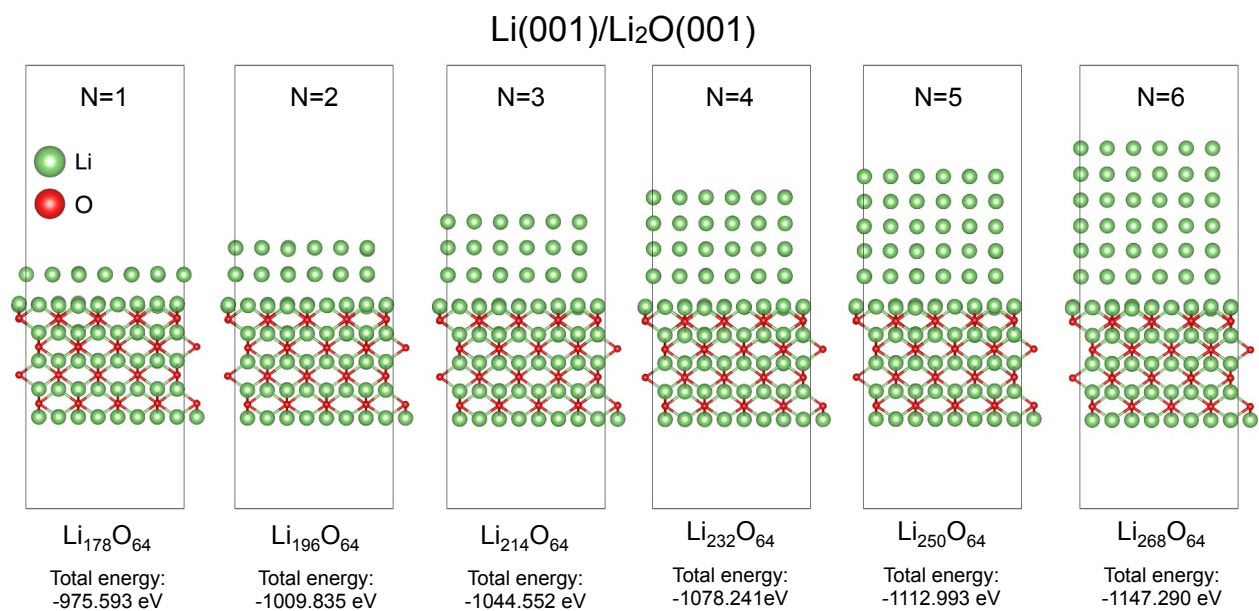


**Figure S3.** Layer-by-layer deposition of Li(001) atoms onto Li<sub>2</sub>O(001) surfaces to compute the plating energy.

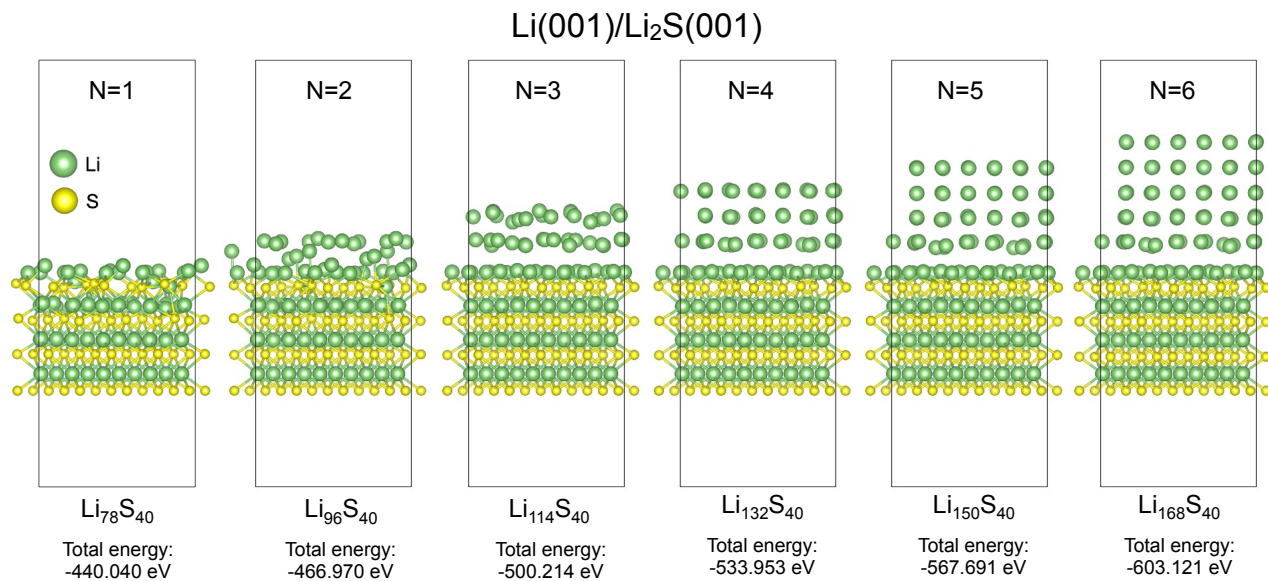


**Figure S4.** Layer-by-layer deposition of Li(001) atoms onto Li<sub>2</sub>S(001) surfaces to compute the plating energy.

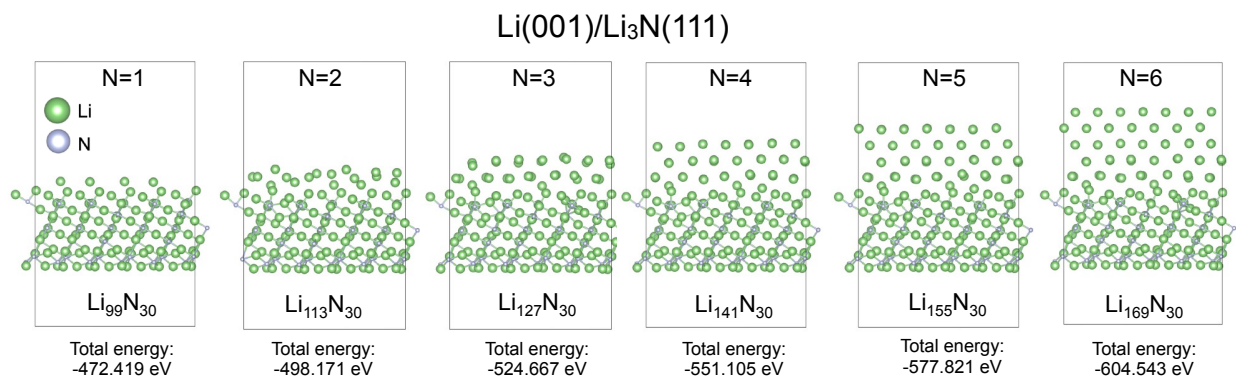


**Figure S5.** Layer-by-layer deposition of Li(001) atoms onto Li<sub>3</sub>N(111) surfaces to compute the plating energy.

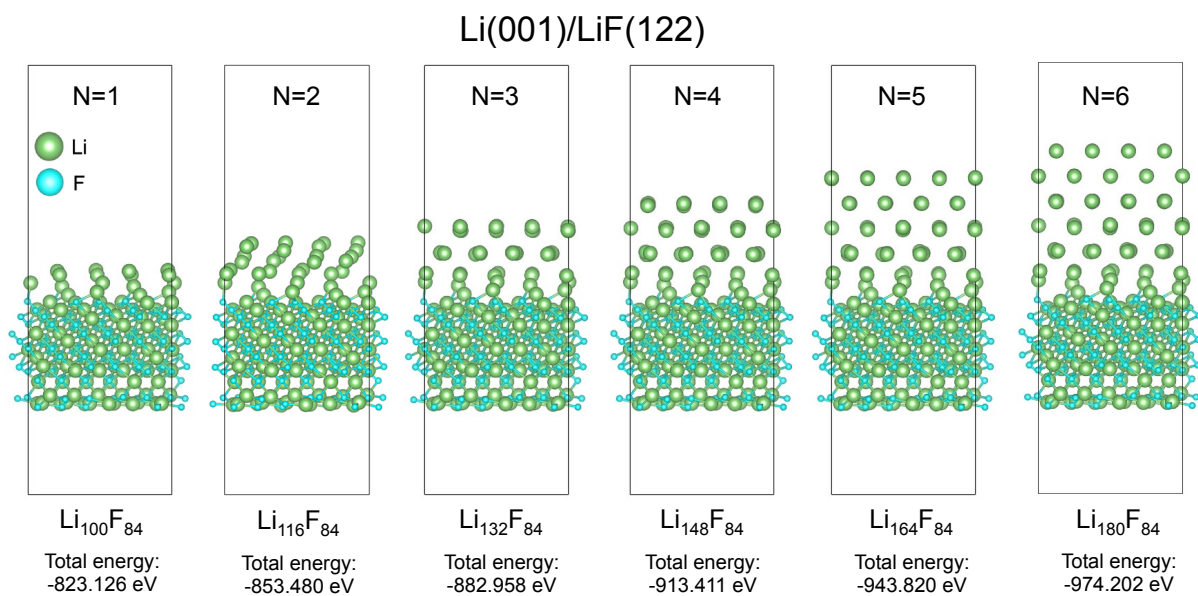


**Figure S6.** Layer-by-layer deposition of Li(001) atoms onto LiF(122) surfaces to compute the plating energy.

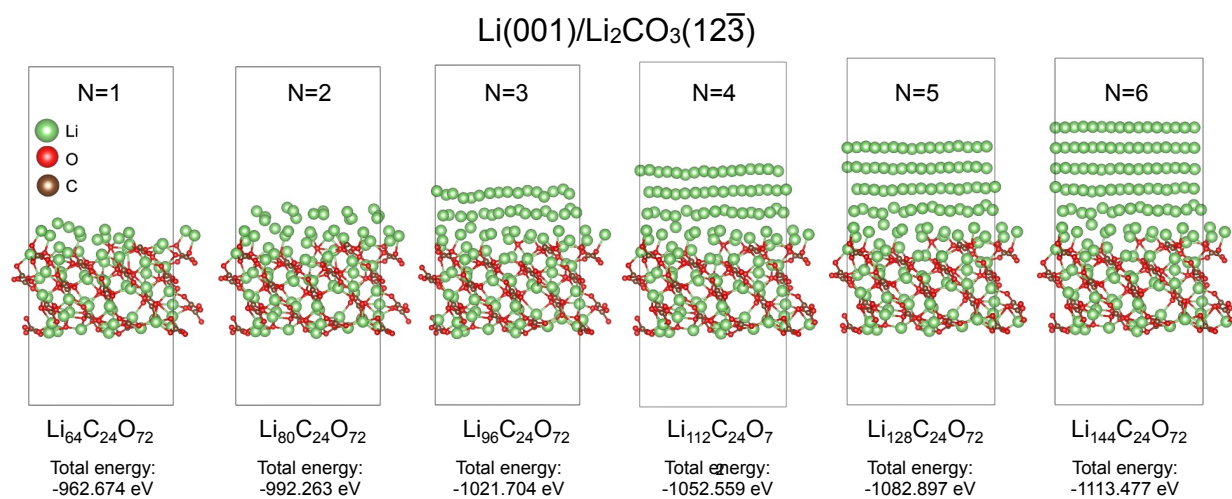


**Figure S7.** Layer-by-layer deposition of  $\text{Li}(001)$  atoms onto  $\text{Li}_2\text{CO}_3(12\bar{3})$  surfaces to compute the plating energy.

### SEI-symmetrized Mg/MgO(111)

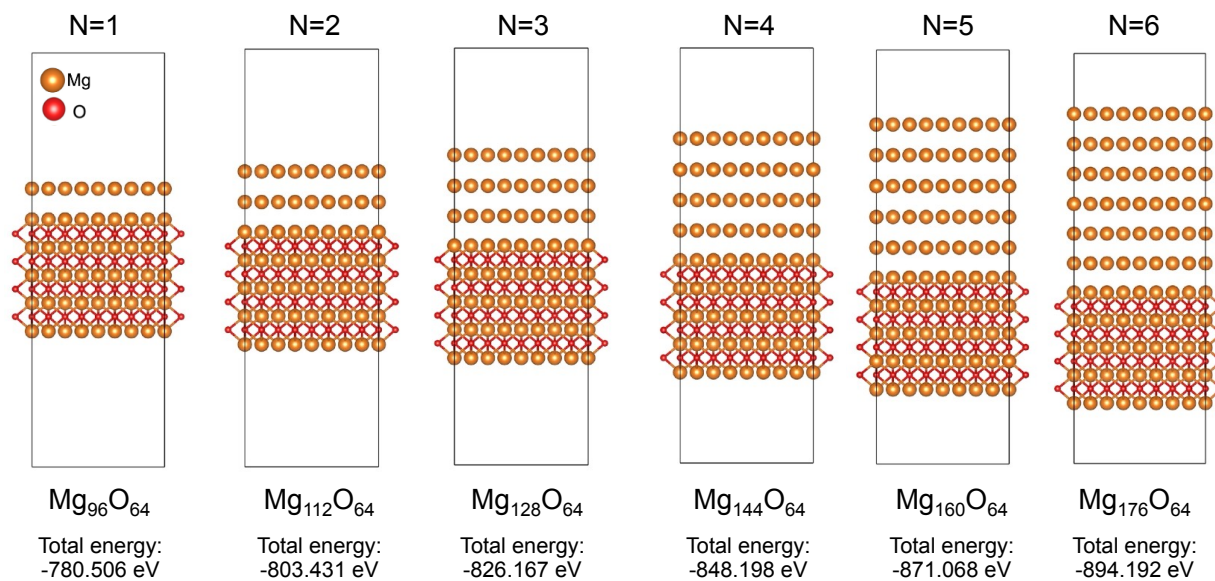


**Figure S8.** Layer-by-layer deposition of Solid Electrolyte Interphase (SEI)-symmetrized Mg atoms onto MgO(111) surfaces to compute the plating energy.

a

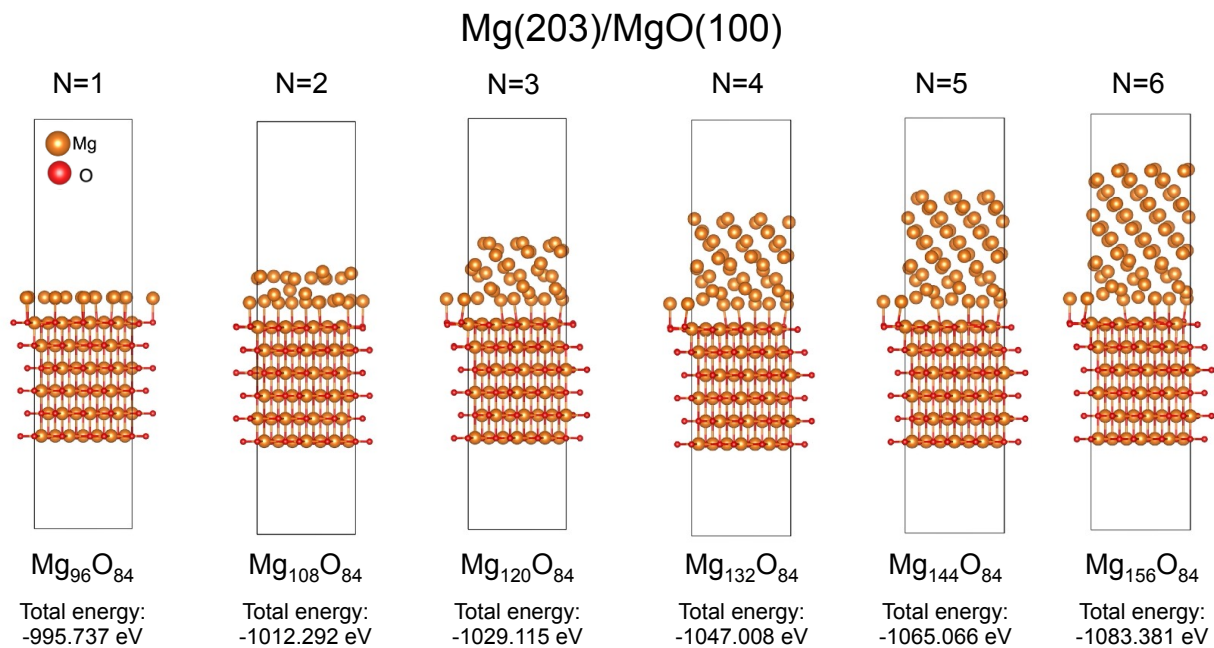


**Figure S9.** Layer-by-layer deposition of Mg(203) atoms onto MgO(100) surfaces to compute the plating energy.

### Mg(001)/MgCl<sub>2</sub>(001)

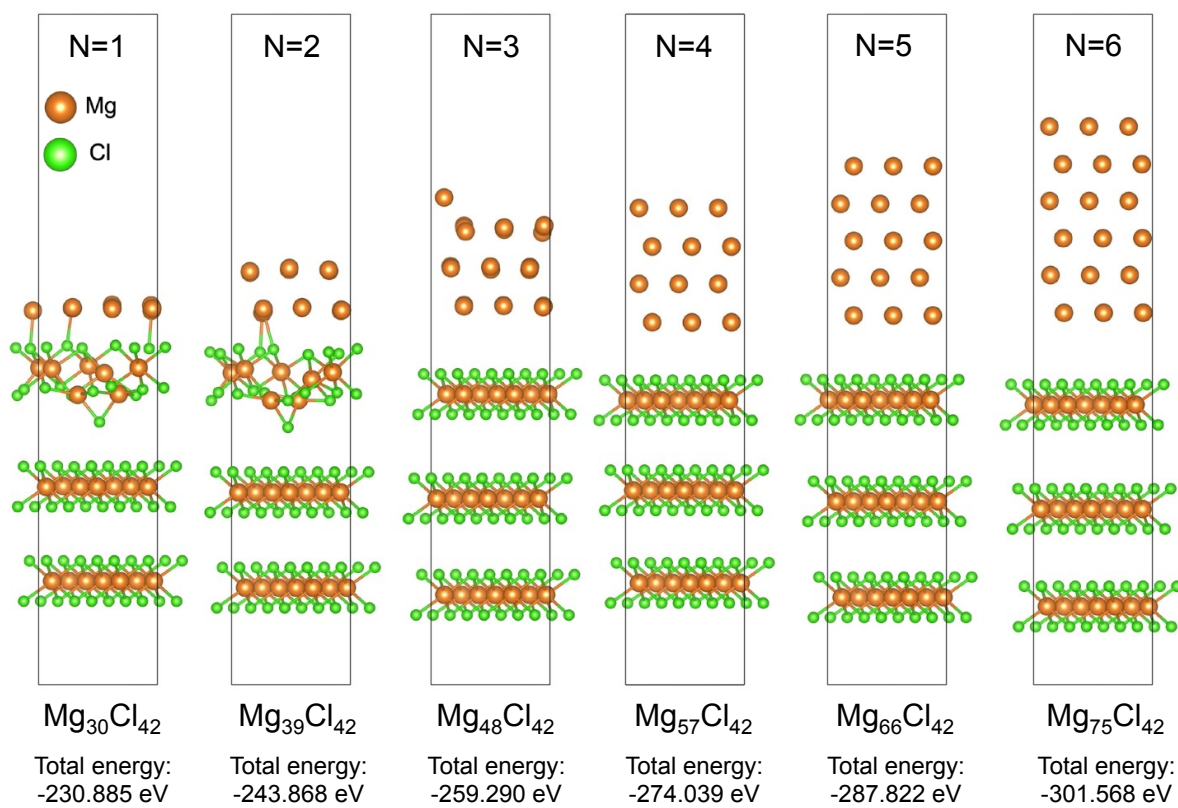


**Figure S10.** Layer-by-layer deposition of Mg(001) atoms onto MgCl<sub>2</sub>(001) surfaces to compute the plating energy.

### Mg(001)/Mg(OH)<sub>2</sub>(001)

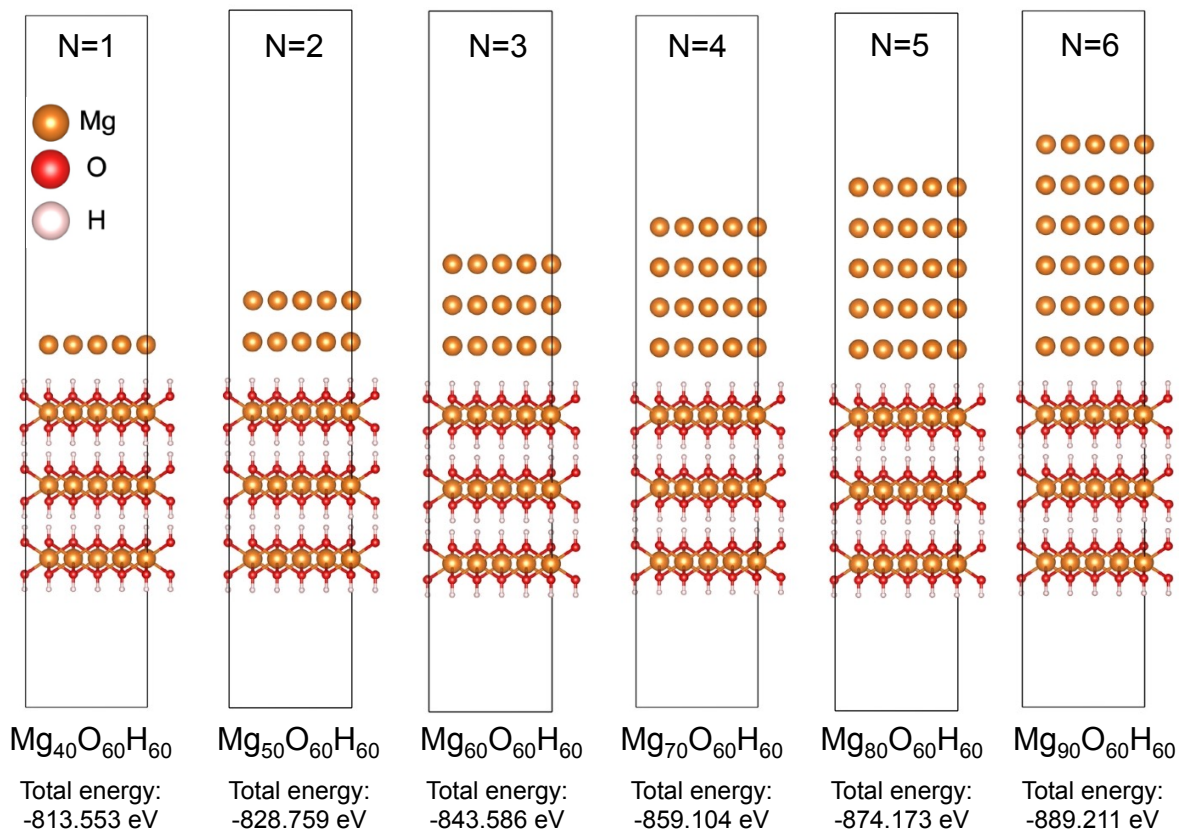


**Figure S11.** Layer-by-layer deposition of Mg(001) atoms onto Mg(OH)<sub>2</sub>(001) surfaces to compute the plating energy.

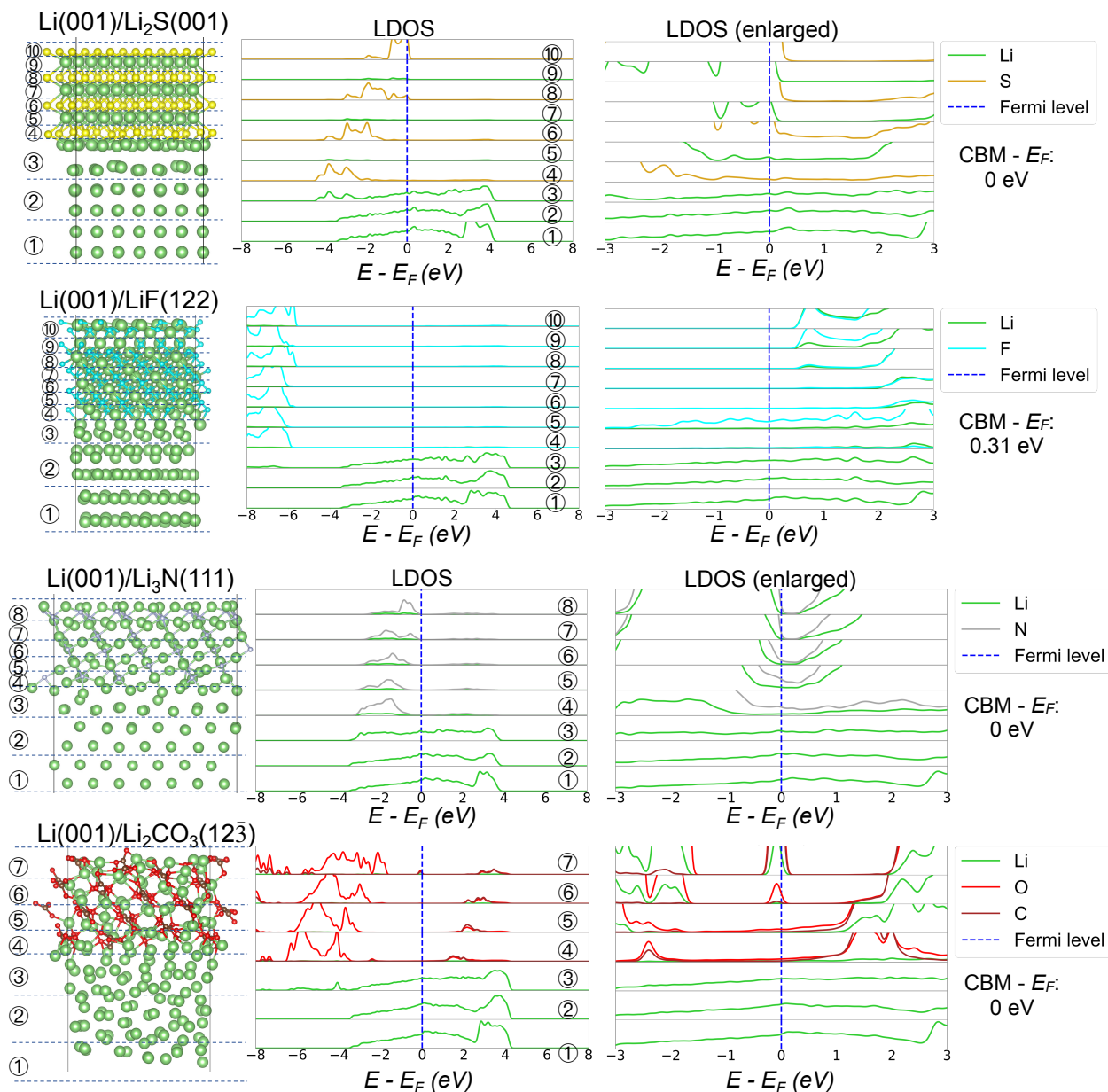


**Figure S12.** Layer-by-layer Local Density of States (LDOS) calculated for heterogeneous interface structures between Li-SEI surfaces and Li(001) anode surface. The atomic structures are aligned with LDOS to depict the corresponding layer LDOS. Each layer in the interface structure is numbered for reference to the layered LDOS. Energy levels ( $E$ ) are referenced to zero at the Fermi level ( $E_F$ ). Enlarged LDOS, with a shorter energy range and reduced intensity range, is provided for enhanced visualization of electronic states around the Fermi level. The difference between the Fermi level and the conduction band minimum (CBM) in the SEI-region ( $CBM - E_F$ ) is also provided.

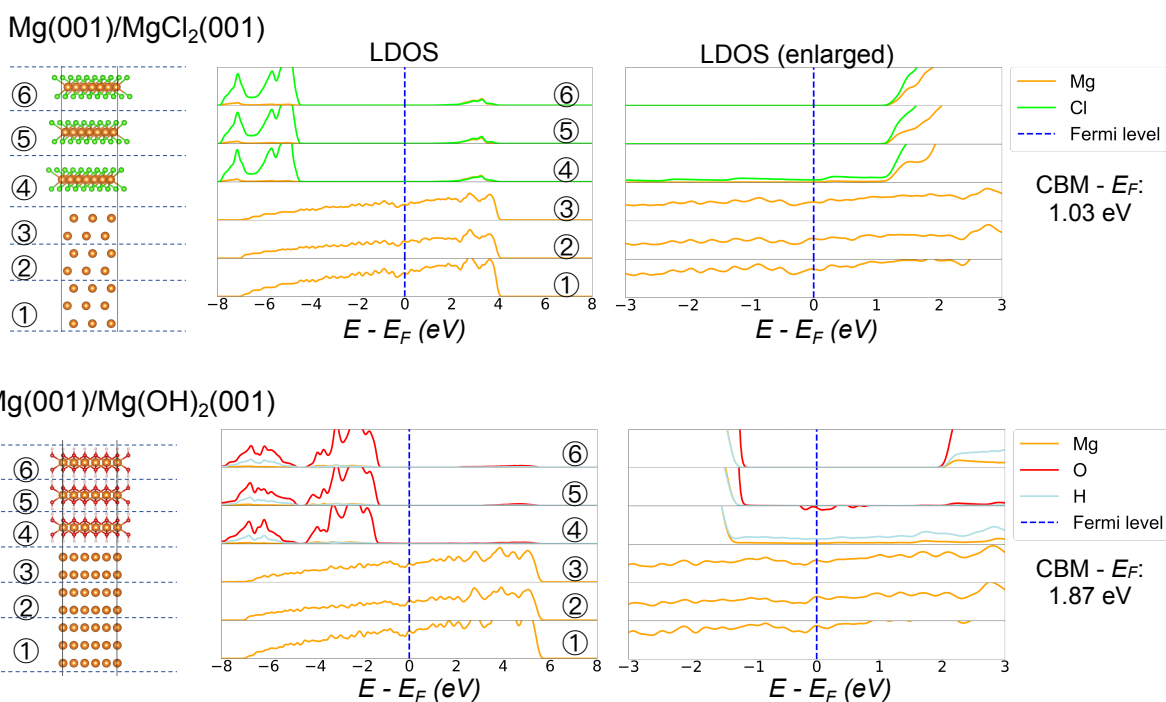


**Figure S13.** Layer-by-layer LDOS calculated for heterogeneous interface structures between Mg-SEI surfaces and Mg(001) anode surface. The atomic structures are aligned with LDOS to depict the corresponding layer LDOS. Each layer in the interface structure is numbered for reference to the layered LDOS. Energy levels ( $E$ ) are referenced to zero at the Fermi level ( $E_F$ ). Enlarged LDOS, with a shorter energy range and reduced intensity range, is provided for enhanced visualization of electronic states around the Fermi level. The difference between the Fermi level and the conduction band minimum (CBM) in the SEI-region ( $\text{CBM} - E_F$ ) is also provided.